Article

Not peer-reviewed version

Chemical Bonding of Nanorod Hydroxyapatite to the Surface of Calciumfluoroaluminosilicate Particles for Improvement of Histocompatibility of Glass Ionomer Cement

Sohee Kang , So Jung Park , Sukyoung Kim , Inn-Kyu Kang *

Posted Date: 25 June 2024

doi: 10.20944/preprints202406.1757.v1

Keywords: bioactivity; calciumfluoroaluminosilicate; glass ionomer cement; histocompatibility; hydroxyapatite; osteoblast

 doi:10.20944/preprints202406.1757.v1

Article

Chemical Bonding of Nanorod Hydroxyapatite to the Surface of Calciumfluoroaluminosilicate Particles for Improving Histocompatibility of Glass Ionomer Cement

Sohee Kang[1], So Jung Park[2], Sukyoung Kim[3] and Inn-Kyu Kang[2*]

[1] Department of Dentistry, Yeungnam University College of Medicine, Daegu 42415, South Korea; kangsh@yu.ac.kr
[2] Department of Polymer Science and Engineering, Kyungpook National University, Daegu 41566, South Korea; ikkang@knu.ac.kr
[3] Materials Science and Engineering, Yeungnam University, Gyeongsan-si 38541, South Korea; sykim@yu.ac.kr
* Correspondence: ikkang@knu.ac.kr

Abstract: This study aimed to enhance the compatibility of glass ionomer cement (GIC) with tooth tissue by chemically modifying its primary component, calciumfluoroaluminosilicate (CFAS), through the incorporation of nanorod hydroxyapatite (nHA). The process involved binding L-glutamic acid to nHA, followed by activation and binding of albumin to create nHA immobilized with albumin. This modified nHA was then used to surface-modify CFAS particles, producing nHA-CFAS powder. The modified powder was mixed with poly(acrylic acid) and UV-cured to form GIC containing nHA-CFAS (GIC-nHA). Fourier transform infrared spectroscopy and scanning electron microscopy were used to confirm the transformation of GIC into GIC-nHA. Cytocompatibility tests with osteoblasts showed that GIC-nHA had superior cell viability and bone formation capabilities compared to the control GIC. The improved histocompatibility is attributed to nHA enhancing the biological activity of osteoblasts, indicating that the surface modification method significantly improves the functional integration of GIC with tooth tissue.

Keywords: bioactivity; calciumfluoroaluminosilicate; glass ionomer cement; histocompatibility; hydroxyapatite; osteoblast

1. Introduction

Glass ionomer cement (GIC) has a variety of uses in dental field, such as being used as a restorative material for primary teeth and as a binder for liners, fissure sealants, and orthodontic brackets [1]. Compared to previously used materials, dental restoration approaches using GIC have been innovatively developed. GIC is composed of a mixture of silica-based inorganic powder and anionic polyacrylic acid. GIC, which exhibits hydrophilicity due to the characteristics of silica powder with many hydroxyl groups, can effectively absorb the liquid remaining at the bottom of the fissure compared to composite resins, thus adhering well to tooth enamel [2]. Although GIC is actively utilized in dental restorations because of its high adhesion to teeth, it is known that there is a need for further improvement in terms of brittleness, abrasion resistance, bending, and tensile strength [3]. The use of nano-sized biomaterials has shown promising potential for the strength, gloss, and aesthetics of dental filling materials in comparison to conventional modifiers [4]. In recent years, there have been many reports focused on improving the mechanical strength of GICs through the introduction of hydroxyapatite (HA) [5]. This is because HA has a chemical structure closely resembles that of human teeth and skeletal systems [6]. Recent advances in HA synthesis technology have made it possible to synthesize HAs of various sizes and shapes [7, 8], facilitating their

 doi:10.20944/preprints202406.1757.v1

application as biocompatible fillers resembling natural teeth. Besides exhibiting unique radiopaque properties [9], HA plays an important role in orthopedic surgery due to its excellent biological activity and osteoconductivity. Furthermore, there has been research on enhancing the antibacterial activity of GIC through the use of HA. Praveen Bali et al. [10] added 8% hydroxyapatite powder to an existing glass ionomer (GC Fuji Type IX gold label, GC Corporation, Tokyo, Japan) and combined it with polyacrylic acid liquid to obtain cylindrical GIC test specimens. They reported that GIC with 8% HA demonstrated higher antibacterial activity than GIC without HA through antibacterial testing using Streptococcus mutans. Haider et al. [11] investigated the topographical effect of HA on the physiological activity of osteoblasts by preparing a nanocomposite. They added spherical HA (sHA) and nanorod HA (nHA) to a PLGA scaffold, respectively. From the results of studying the interaction between the nanocomposite and osteoblasts, they concluded that the nanorod HA-containing scaffold further promotes the bioactivity of osteoblasts. In this study, nHA was chemically bonded to the surface of calcium fluoroaluminosilicate (CFAS), a solid component of GIC, using biocomponents L-glutamic acid (G) [12] and albumin (Alb) as spacers. The progress of the surface reaction was confirmed through ATR-FTIR and FE-SEM. The resulting CFAS-nHA powder was mixed with polyacrylic acid and UV cured to prepare a disk-shaped GIC-nHA. The cytocompatibility and bone formation ability of GIC and GIC-nHA discs were investigated using osteoblasts.

2. Materials and Methods

2.1. The preparation of Materials

For this experiment, the following materials were purchased from Sigma Aldrich Chemical Company in the United States and used: 3-Aminopropyltriethoxysilane (A), L-glutamic acid, N-(3-dimethylaminopropyl)-N'-ethylcarbodiimide hydrochloride (EDC), N-hydroxysuccinimide (NHS), fluorescein isothiocyanate (FITC), and bovine serum albumin. nHA was synthesized according to the details provided in a previous study [11]. The mouse pre-osteoblast cells (MC3T3-E1), purchased from the Korea Cell Bank located in Seoul, South Korea, and were restored in liquid nitrogen before cell seeding. A phosphate-buffered saline (PBS) solution (pH 7.4) was also acquired from Sigma-Aldrich Chemical Company , which contains Na2HPO4, KH2PO4, NaCl, and KCl. CFAS, a solid powder used in the preparation of GIC, was provided by Professor Sukyoung Kim of Yeungnam University, Korea, and nHA was chemically bonded to the surface of CFAS to be used as a solid component of GIC. The liquid component of GIC (GC International, Japan, GC Fuji II LC) was used as the polyacrylic liquid component for preparing GIC. The MC3T3-E1 cells were cultured in α-minimum essential medium (α-MEM) supplemented with 10% fetal bovine serum and 1.0% penicillin G-streptomycin at a temperature of 37°C. Under A 5% CO_2 atmosphere, the culture medium was replaced every alternate day. By scanning electron microscope (FE-SEM, Hitachi S-400, Tokyo, Japan), the presence of nHA on the surface of the solid particles was observed.

2.2. Synthesis and Surface Modification of CFAS

We used the sol-gel method of Khiri et al. [13], to prepare CFAS. The composition of ingredients used to prepare CFAS is shown in Table 1. Initially, 23.89 ml of tetraethylorthosilicate was dissolved in 400 ml of ethanol. Subsequently, an aqueous solution (100 ml) containing aluminum nitrate, calcium nitrate, and ammonium dihydrogen phosphate was added drop-wise. Finally, rapid addition of fluorosilicic acid followed by stirring the mixture at 80°C for 4 hours resulting in the formation of a gel-like product. The gel was then dried for 24 hours at a temperature of 80°C and then heat-treated for 10 minutes at a temperature of 750°C. After the heat treatment, the sample was quenched in water, powdered, and sieved to obtain a micrometer-sized sample (Figure 1).

 doi:10.20944/preprints202406.1757.v1

Table 1. Feed ratio of calciumfluoroaluminosilicate microparticles.

Ingredient	Chemical formular	Molar ratio	50 mmol (amount used in the experiment)
Tetraethylorthosilicate	$Si(OC_2H_5)_4$	2.133	23.89 ml
Ammoniumdihydrogen phosphate	$NH_4H_2PO_4$	0.160	0.92 g
Fluorosilicic acid	H_2SiF_6	0.167	2.95 ml
Aluminum nitrate	$Al(NO_3)_3$	2.200	41.27 g
Calcium nitrate	$Ca(NO_3)_3$	1.000	11.81 g

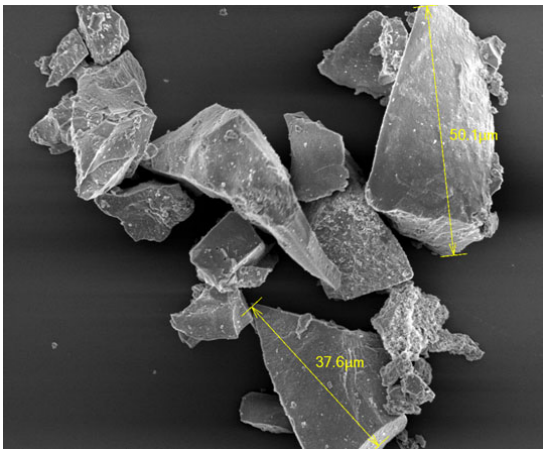

Figure 1. SEM image of calciumfluoroaluminosilicate (Silicate) microparticles prepared in this study.

To incorporate primary amino groups to the surface of CFAS particles, a mixture of aminopropyltriethoxysilane (A) and distilled water in a 1:9 ratio was prepared, and 0.06 g of CFAS was added to the mixture. Then, it was subjected to ultrasonic machine for 30 minutes. Subsequently, the acetic acid was applied to set the pH of the reaction solution to 4.5 - 5.0. The reaction solution was maintained at 90°C for 2 hours while flowing nitrogen was flowed through. The reactants was then transferred to distilled water and ultra-sonicated for 5 minutes to remove unreacted A. The resulting CFAS with immobilized A (CFAS-A) was dried under reduced pressure for 12 hours at a temperature of 25°C.

2.3. Surface Modification of nHA

As a result of TEM examination of nHA synthesized according to a previously reported method [11], it was rod-shaped with a length of 30 to 150 nm (Figure 2). The nHA particles exhibit numerous hydroxyl groups on their surface [13, 14]. In this study, our aim is to chemically bind nHA particles to the surface of CFAS microparticles through a chemical reaction. These solid-solid reactions have low reactivity because they occur in a heterogeneous system [15]. To increase the surface reactivity of nHA particles and improve their dispersibility in aqueous solution, albumin was chemically coupled to the nHA surface. The carboxyl group present in the side chain of the introduced albumin molecule was used for reaction with CFAS particles (Figure 3). For this purpose, nHA-G (nHA into which L-glutamic acid was introduced) was first prepared by reacting L-glutamic acid with hydroxyl groups on the surface of nHA [16]. L-glutamic acid was dissolved in an aqueous solution at pH 5. Then, 1-ethyl-3-(3-dimethylaminopropyl) carbodiimide hydrochloride (0.5 g, 0.25 wt%) and N-hydroxysuccinimide (0.5 g, 0.25 wt%) was added and stirred for 4 hours at room temperature,

 doi:10.20944/preprints202406.1757.v1

resulting in the activation of the carboxyl group of L-glutamic acid. Next, 0.5 g of nHA was added and stirred for 24 hours. Finally, the reaction solution was centrifuged to form a precipitate. After washing the precipitate three times with deionized water, it was lyophilized to obtain nHA-G [16].

The resulting nHA-G was mixed with distilled water, stirred for 1 minute, and left to stand. As a result of observing the solution, no precipitate was observed with the naked eye. This is because L-glutamic acid binds to nHA, thereby improving dispersibility in aqueous solution. Despite the improved dispersibility of nHA, to increase its reactivity with micro-sized CFAS solid particles, the spacer introduced on the nHA surface must be sufficiently long and dynamically mobile in the aqueous solution [17]. Therefore, we attempted to bind water-soluble albumin to the surface of nHA-G as a second spacer. We dissolved 0.06 g albumin, acting as a chain extender, in 100 mL of deionized water. Thereafter, 0.1 g each of EDC and NHS was added and stirred for 2 hours at a temperature of 25°C, resulting in the activation of the carboxyl group of albumin. Then, we added 0.5 g of nHA-G particles in the albumin solution, and the mixture was reacted for 24 hours. The reaction solution was placed in a semi-permeable membrane (MWCO: 100,000) and dialyzed to separate un-reacted albumin. It was then washed three times with deionized water. The resulting product is called albumin-immobilized nHA (nHA-Alb). Albumin immobilized on the nHA surface in an aqueous solution not only exhibits dynamic motion but also contains several carboxyl groups. Therefore, it is expected that the probability of a chemical bond forming between the primary amino group of A, immobilized on the CFAS surface, and the albumin immobilized on nHA increases. The ATR-FTIR spectra of albumin chemically bound to the nHA particle surface and nHA-Alb chemically bound to the CFAS surface were examined using a Galaxy 7020A device (Mattson, Fremont, CA, USA).

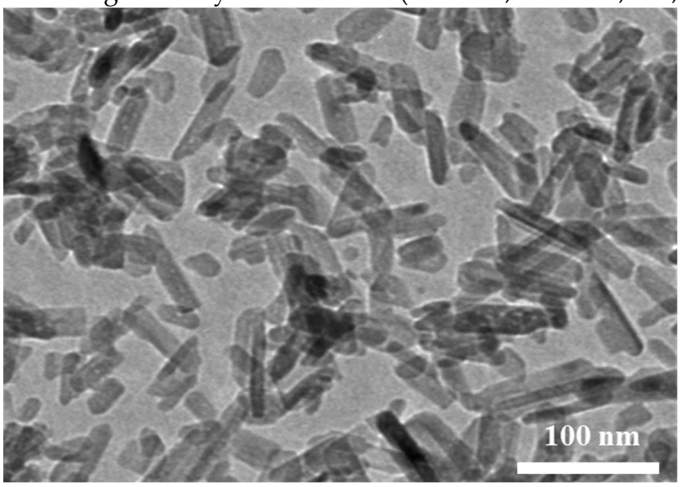

Figure 2. TEM image of nHA used in this study synthesized by chemical precipitation method (Reference 11 is cited for the picture).

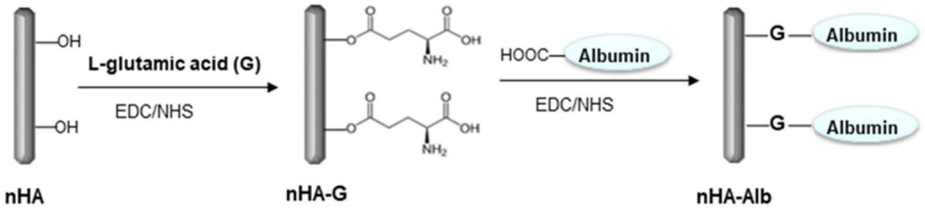

Figure 3. Schematic diagram showing the surface modification of nHA using L-glutamic acid and albumin as linkers.

2.4. Chemical Bonding of nHA to the CFAS Surface

The chemical bonding of nHA-Alb to CFAS-A was performed as follows (Figure 4): 0.5 g of nHA-Alb was added to a 100 mL aqueous solution containing 0.5 g of EDC (0.25 wt%) and 0.5 g of NHS (0.25 wt%). By stirring at 25°C for 6 hours, the carboxyl group of albumin was activated. Then, CFAS-A was added to the aqueous solution and stirred mechanically for 24 hours. The reaction mixture

 doi:10.20944/preprints202406.1757.v1

was then centrifuged at 1200 rpm for 10 minutes to precipitate CFAS-nHA. Distilled water was added to the precipitate, and centrifugation was repeated to remove any unreacted activators. The introduction of nHA into CFAS was confirmed through ATR-FTIR spectrum analysis. Additionally, the surface morphology of CFAS-nHA was analyzed using FE-SEM micrographs (Hitachi 400, Tokyo, Japan).

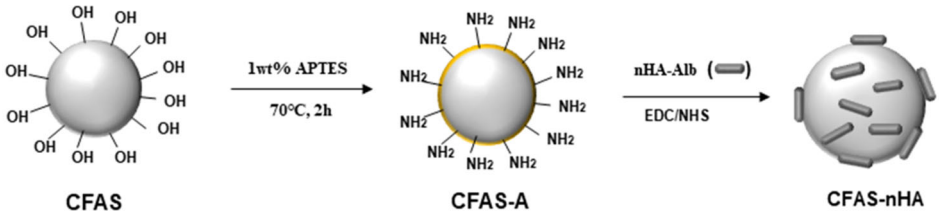

Figure 4. Schematic diagram showing the chemical bonding of nHA on the surface of CFAS microparticles.

2.5. Preparation of GIC-nHA discs

GIC-nHA discs were prepared as follows (Figure 5). 0.5 Gram of CFAS-nHA was placed on a paper mixing pad, and a commercially available liquid component (2 ml) of GIC (GC International, Japan, GC Fuji II LC) was added dropwise and mixed. After mixing for 5 minutes, transfer to a 24-well culture dish and flatten. After that, LED Spotlights–470nm Blue were irradiated for 10 minutes to proceed with photopolymerization to manufacture a GIC-nHA disk. Meanwhile, a control sample was prepared by photopolymerization in the same manner using 0.5 g of CFAS and a liquid component (2 ml) of GC Fuji II LC.

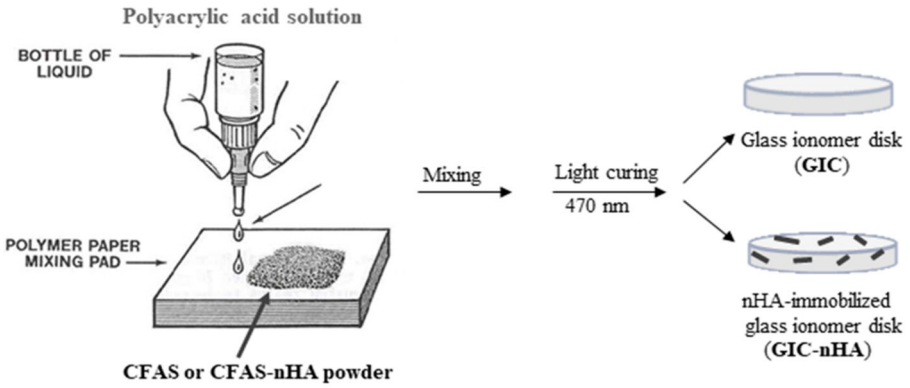

Figure 5. Schematic diagram showing the manufacturing process of glass ionomer disc using polyacrylic acid and surface-modified silicate powder.

2.6. Cytocompatibility of GIC-nHA

By using standard protocol, we investigated the adhesion, proliferation, and osteogenic characteristics of MC3T3-E1 cells, confirming the effects of incorporating nHA into GIC.

2.6.1. Cell Adhesion

We evaluated the cellular response of MC3T3-E1 cells (4 x 10^4 cells/mL) on disk surfaces by seeding them onto GIC and GIC-nHA discs. The cells were cultured in a humidified atmosphere for 24 hours using α-MEM. After removing the supernatant, the cells were washed with PBS and fixed with a 2.5% glutaraldehyde solution for 10 minutes. Subsequently, the samples underwent dehydration and drying procedure using a critical point dryer. Before capturing SEM image, they were sputter-coated with gold.

2.6.2. MTT Assay

 doi:10.20944/preprints202406.1757.v1

MC3T3-E1 cells were cultured on GIC and GIC-nHA discs for 3 days. Afterwards, the viability of the cells was measured through MTT assay. This assay relies on the reduction of MTT, a yellow water-soluble tetrazolium dye, primarily by the mitochondrial dehydrogenases, to purple colored formazan crystals [18]. For MTT analysis, sterilized disc samples were plated in 24-well dishes, 500 µL of non-osteogenic α-MEM was added, and MC3T3-E1 cells were seeded onto each disk at a density of 1.2×10^4 cells/cm^2. After 3 days of culture, the removal of the supernatant and two subsequent washes of the scaffold by PBS solution were conducted sequentially. Cell-seeded scaffolds were cultured in 500 µL of MTT solution (500 µg/mL) at 37 °C for 4 h, followed by the removal of the supernatant. The generated purple formazan crystals were dissolved for 10 minutes using 250 µL of dimethyl sulfoxide. Wells injected with MC3T3-E1 cells without discs served as the positive controls, while empty wells without cells were used as the negative controls. The absorbance of extract was recorded at 570 nm based on 690 nm for the medium using Symergy HT multidetection microplate reader (Symergy HT, BioTek, USA). The amount of generated formazan was determined by using microplate reader data. Data from the negative controls were subtracted from the measurements. The number of viable cells was correlated with the optical density, and cell viability was assessed by normalizing the value to that of the positive control wells.

2.6.3. Cytotoxicity

The cytotocity of GIC and GIC-nHA was evaluated by seeding cells at a density of 2.0×10^4 cells/mL onto both discs. The discs were then incubated in the Dulbecco's Modified Eagle Medium (DMEM) at 37°C in a 5% CO_2 atmosphere for 1 and 2 days. Afterwards, 5 µL of calcein-AM (4 mM in anhydrous DMSO) and 20 µL of ethidium homodimer III (2 mM in DMSO/H_2O) were added to 10 mL of PBS solution and thoroughly mixed to prepare the staining solution, which was then used to stain the cells [16]. After removing the DMEM from the culture wells, both GIC and GIC-nHA discs were washed with PBS solution for two times. Then, a large amount of the staining solution was added to fully cover the cells. The discs were subsequently incubated in a dark area at room temperature for additional time. After 30 minutes, the staining solution was removed, and the cells were washed with PBS solution for three times. Finally, the cells were preserved in PBS solution until observation with a confocal laser scanning microscope. Live and dead cells were simultaneously assessed at calcein-AM (494 nm excitation wavelength) and ethidium homodimer III (530 nm excitation wavelength).

2.6.4. Actin Cytoskeleton Assay

Osteoblast cells were seeded onto GIC discs at a concentration of 2×10^4 cells/ml and cultured for 3 days. Next, 4% paraformaldehyde solution was used to fixe the cells. The cells were then washed with PBS solution containing 0.05% Tween-20. Subsequently, the samples were permeabilized with 0.1% Triton X-100 in PBS solution for 15 minutes at 25°C. Following permeabilization, the samples were incubated in a mixture of 1% bovine serum albumin (BSA) and PBS solution for 30 minutes. After washing the cells 2-3 times with PBS solution, TRITC-conjugated phalloidin (Millipore, Cat. No. 90228) solution was added and incubated at room temperature for 30 minutes. Finally, a confocal laser scanning microscope (CLSM, model 700, Carl Zeiss) was utilized to capture the fluorescence images [19].

2.6.5. von Kossa Assay

Through the von Kossa assay, we aimed to assess the calcium deposition response of MC3T3-E1 cells cultured on GIC and GIC-nHA discs. MC3T3-E1 cells were seeded in 24-well culture plates at a density of 5×10^4 cells/mL and cultured for 14 days in α-MEM at 37°C in a humidified atmosphere of 5% CO_2. After gently washing both disks three times with PBS solution for 5 minutes each, they were fixed with 10% formaldehyde for 30 minutes. Afterward, each disc was washed three times with distilled water for 10 minutes each, followed by treating with 5% $AgNO_3$ solution and exposure to UV irradiation for 5 minutes. The GIC disks were washed twice with PBS to remove remaining

 doi:10.20944/preprints202406.1757.v1

$AgNO_3$ and soaked in 5% $Na_2S_2O_3$ solution for 5 minutes. Finally, after washing the GIC disks two times with distilled water, digital images of the stained cells were captured using an optical microscope equipped with a camera (Nikon E 4500, Japan) [18].

2.7. Statistical Analysis

The experiments were performed in triplicates, and all datas were expressed as the means ± standard deviation. Statistical analysis was conducted using Student's two-tailed test along with Scheffe's test for multiple comparison statistics. A p-value less than 0.05 is considered to be statistically significant.

3. Result

3.1. Immobilization of nHA on CFAS particle surface

ATR- FTIR is a recommended method to confirm whether biomolecules such as amino acids or proteins have been introduced to the surface of solid particles such as CFAS or nHA [20]. Figure 6 shows the results of ATR- FTIR measurements after surface modification of nHA and CFAS. The infrared spectrum of the nHA sample showed typical apatite modes near 1086, 1021, 961, 600 and 562 cm^{-1} [20]. Looking at the FT-IR spectrum of nHA-Alb obtained by binding L-glutamic acid to nHA and then binding to albumin, the carbonyl stretching vibration of the ester formed by the reaction between the hydroxyl group of nHA and the carboxyl group of L-glutamic acid appears at 1707 cm^{-1}. Furthermore, peaks attributed to amide I and II of the introduced albumin appeared at 1647 cm^{-1} and 1545 cm^{-1}, respectively [21]. In the IR spectrum of CFAS-nHA, the characteristic peak of nHA-Alb appeared, indicating that nHA was successfully chemically bonded to the CFAS surface (Figure 6).

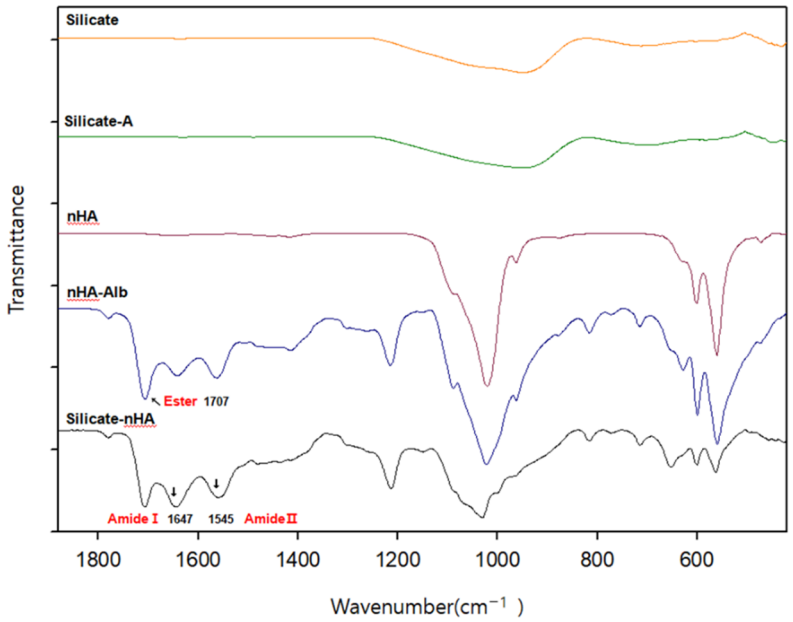

Figure 6. ATR-FTIR spectra of albumin-bound nHA (nHA-Alb) and nHA-bound CFAS (CFAS-nHA).

Figure 7 shows SEM images of CFAS surface before (a) and after (b) chemical bonding of nHA. It can be seen that the CFAS surface shows a nanoporous structure (Figure 7a), whereas the CFAS-nHA surface has nanorod nHA bound to the surface (Figure 7b). As such, nHA bound to the CFAS surface is expected to play a major role in improving histocompatibility when used as a filling material for tooth hard tissue [22].

 doi:10.20944/preprints202406.1757.v1

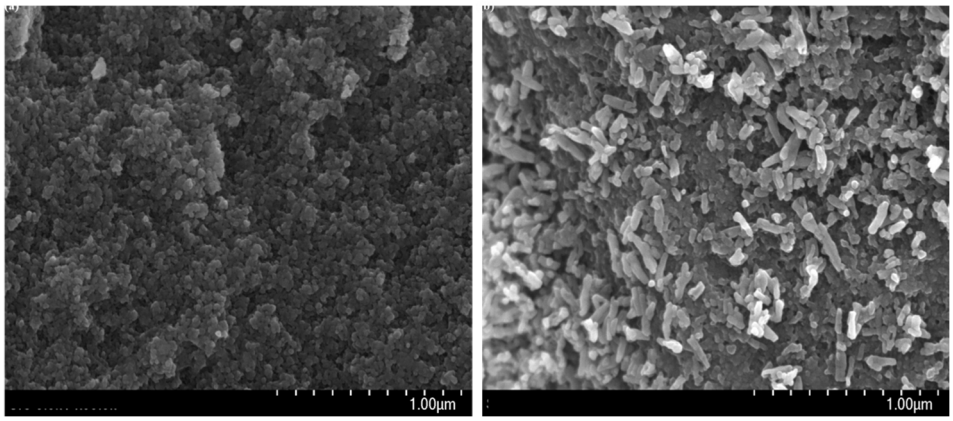

Figure 7. Scanning electron microscope (SEM) images of CFAS microparticles before (a) and after (b) chemical bonding of nHA.

3.2. Cytocompatibility of GIC-nHA

GIC was prepared using CFAS and polyacrylic acid. In addition, GIC-nHA was prepared using CFAS-nHA and polyacrylic acid. After culturing the osteoblasts on the above two samples for 24 hours, they were observed by SEM. As shown in Figure 8, osteoblasts were well spreading on the GIC (Figure 8a) and GIC-nHA(Figure 8b) samples after 24 hours.

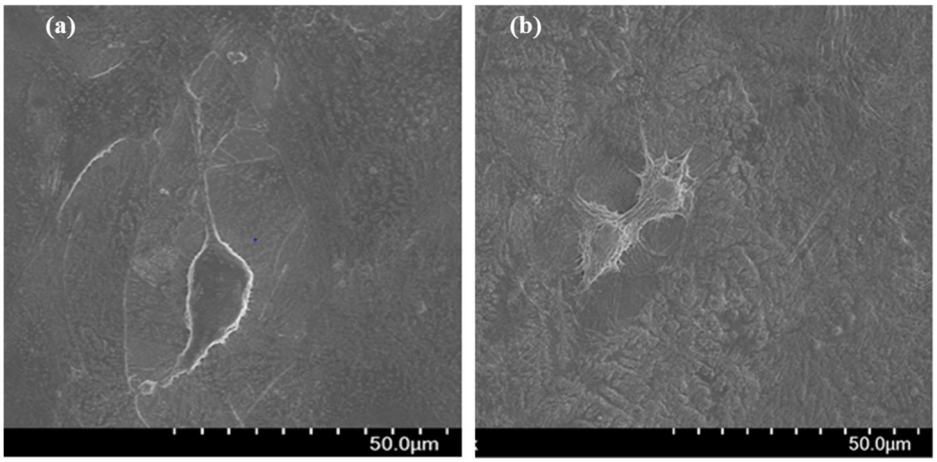

Figure 8. SEM images of osteoblasts cultured for 24 h in GIC (a) and GIC-nHA (b).

Osteoblasts were cultured in GIC and GIC-nHA samples for 24 and 48 hours, then stained using calcein-AM and ethidium Homodimer III dye, and the results are shown in Figures 9 and 10. As a result, no red fluorescence image appeared in the GIC and GIC-nHA samples. These results indicate that both GIC and GIC-nHA samples do not exhibit toxicity. Additionally, as shown in Figure 10, the number of cells attached to GIC-nHA was much higher than that of cells attached to GIC. This is believed to be because CFAS-nHA introduced into GIC promoted cell proliferation.

 doi:10.20944/preprints202406.1757.v1

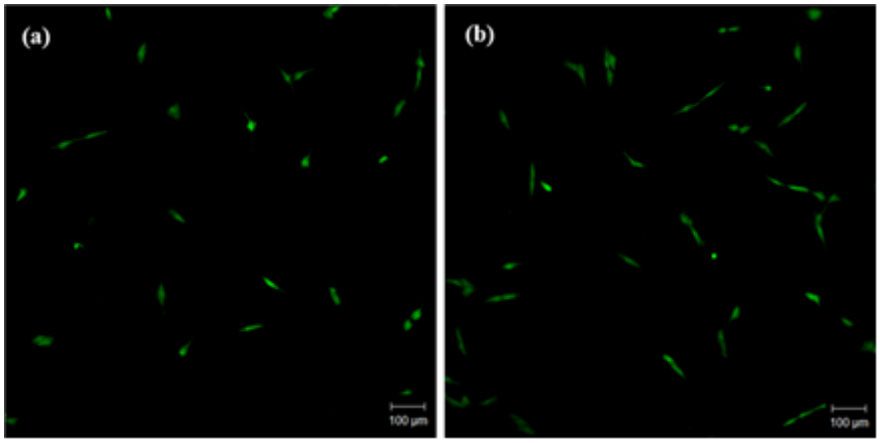

Figure 9. Live and dead assay of MC3T3 E1 cells which were cultured for 24 hours on the GIC and the GlC-nHA. Cells were stained with calcein AM and ethidium homodimer III. Initial cell number = 1.2 ×10⁴/ml.

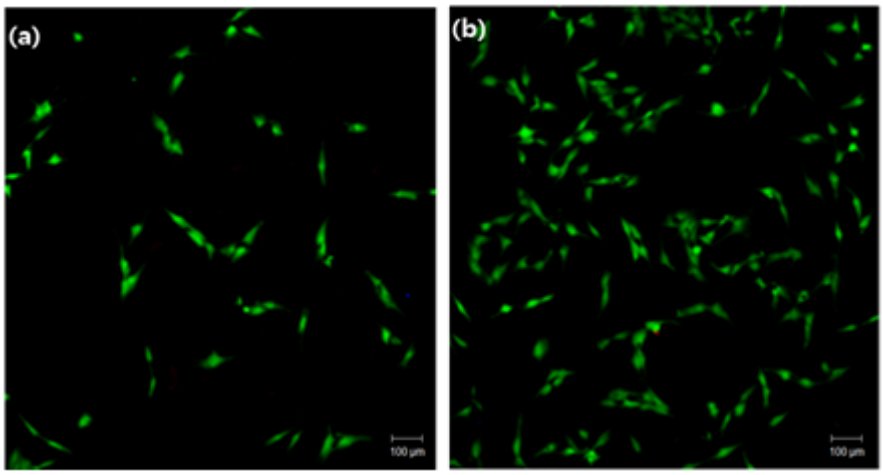

Figure 10. Live and dead assay of MC3T3 E1 cells which were cultured for 48 hours on the GIC and the GlC-nHA. Cells were stained with calcein AM and ethidium homodimer III. Initial cell number = 1.2 ×10⁴/ml.

MC3T3 E1 cell proliferation in GIC and GIC-nHA was assessed using the MTT assay [23]. According to the MTT analysis, the proliferation rate of MC3T3-E1 cells cultured on the GIC-nHA sample for 3 days was significantly higher than the that on the GIC (Figure 11). This result indicates that the immobilization of nHA on the surface of CFAS not only enhances adhesion, but also provides better opportunities for cell proliferation. This might because the nHA can act as an authentic extracellular matrix.

 doi:10.20944/preprints202406.1757.v1

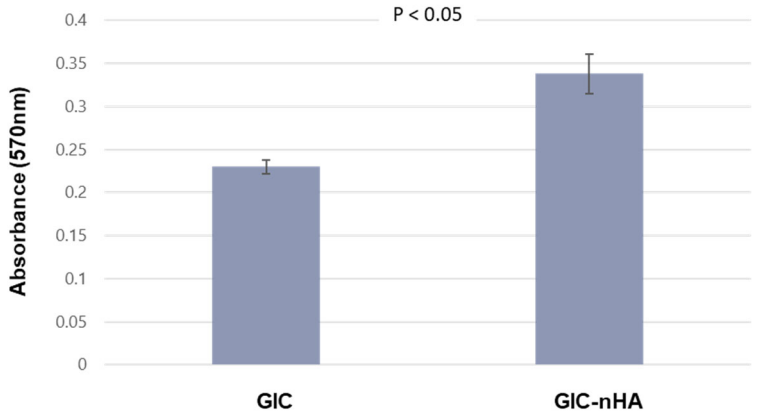

Figure 11. MTT assay of MC3T3 E1 cells cultured for 3 days on GIC and GIC-nHA under α-MEM. Initial cell concentration: 1.2×10^4/ml.

The actin microfilament, which constitute the cytoskeleton of the cells, play crucial role in cellular processes, cell shape determination, and cell attachment pattern. When cells attach to the extracellular matrix, they form filopodia. They are guided into position by actin, interacting with the plasma membrane [24]. Figure 12 shows confocal microscopy images of osteoblasts on GIC (a) and GIC-nHA (b) discs. Results suggest that osteoblasts in both GIC and GIC-nHA exhibit a highly organized cytoskeleton.

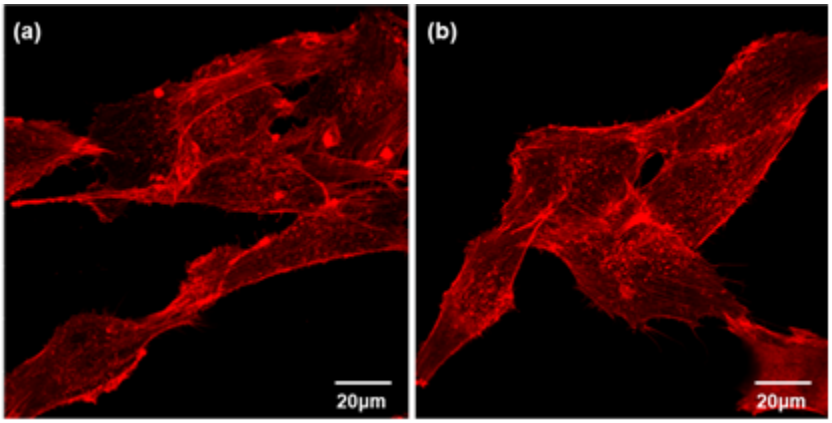

Figure 12. Confocal microscopy images of the actin filaments of osteoblasts cultured for 3 days on GIC (a) and GIC-nHA (b). (magnification × 400).

Figure 13 shows the results of Von Kossa analysis performed after culturing osteoblasts in GIC and GIC-nHA samples for 14 days. Bone nodules are considered as specific markers for osteoblast differentiation. In von Kossa analysis, calcified areas stain as black spots. According to the von Kossa analysis, more bone nodule formation was observed in GIC-nHA (Figure 13b), compared to GIC (Figure 13a). These results indicate that hydroxyapatite triggers and accelerates osteoblast differentiation [25].

 doi:10.20944/preprints202406.1757.v1

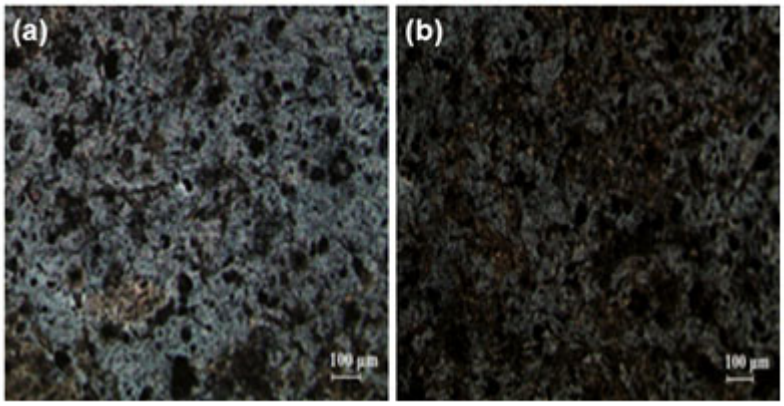

Figure 13. von Kossa staining of osteoblast cells cultured on GIC (a) and GIC-nHA for 14 days. The calcium containing areas are stained as black in color.

4. Discussion

Glass Ionomer Cement (GIC) has been recognized as an ideal dentin substitute due to its ability to exhibit antidental properties, provide stable ionic bonds, and aid in the remineralization process. Initially developed for grade 5 cavity restorations, GIC is now being expanded for use as permanent adhesives, bases, grade 1 and 3 fillings, and core and fissure sealants. To be effective as a dental filling material, GIC must withstand high loads. Many studies have aimed to improve the mechanical properties of GIC composed of polyacrylic acid-based resin and silica-based inorganic particles [26,27,28]. However, while numerous studies have examined the mechanical properties of GIC in direct contact with enamel or dentin, few have reported on the tissue compatibility of GIC. Since silica-based inorganic powder, a key component of GIC, differs chemically from enamel or dentin, long-term tissue compatibility between GIC and teeth is crucial.

Hydroxyapatite (HA) is an inorganic mineral found in bones and teeth, contributing to structural strength and bone regeneration. There has been a study to improve the histocompatibility of GIC by introducing HA into the inorganic solid powder of glass ionomer. Noorani et al. [29] investigated cytotoxicity using GICs containing 5% HA-SiO2, Fuji IX GP, and encapsulated Fuji II LC. Fuji IX GP exhibited the lowest cytotoxicity, HA-SiO2-GIC showed medium toxicity, and Fuji II LC had the highest toxicity, attributed to residual unreacted monomers [30]. The study suggested that the 5% HA-SiO2 introduction into GIC was insufficient to effectively suppress toxicity. Another study increased the affinity of implants to bone by manufacturing hydroxyapatite in nano-size and immobilizing it on the surface of implants such as metal or ceramic. Kwon et al. [31] reported that immobilization of nHA and simvastatin on titanium surfaces improved bone formation and osseointegration in vitro and in vivo. Surface-treated pristine Ti using NaOH, 1,1-carbonyldiimidazole, β-cyclodextrin-immobilized nHA powder, and simvastatin enhanced osteogenic differentiation of MC3T3-E1 cells in vitro. Additionally, nHA and simvastatin-fixed screw titanium improved bone formation between the screw and host bone in rabbit models. The study concluded that surface modification with nHA and simvastatin is an effective tool for developing dental implants. Kim et al. [32] prepared zirconia screws and discs by hot press injection molding using granular zirconia (200–500 nm in diameter). To increase the physiological activity of the zirconia implant, nHA (20-70 nm in diameter) and type I collagen were chemically bonded to the surface. Cytotoxicity and differentiation experiments using osteoblast cells showed that the modified zirconia implants were non-toxic and had high differentiation potential.

In this study, nHA was chemically bonded to the surface of CFAS, a silica-based inorganic component. The obtained CFAS-nHA was mixed with the GIC liquid component of Fuji II LC (GC International, Japan) and cured with UV light to prepare GIC-nHA with improved tissue compatibility. By chemically bonding nHA to the surface of micro-sized inorganic powder used for manufacturing GIC, the osteoblast-activating ability of nHA can be utilized while maintaining the mechanical properties of GIC. Both nHA and CFAS are solid components that readily precipitate

 doi:10.20944/preprints202406.1757.v1

from aqueous solutions. To chemically link these two solid components, a linker must first be immobilized on each solid surface. Initial experiments combining L-glutamic acid with nHA and reacting it with CFAS-A were unsuccessful, likely due to low dispersibility and steric hindrance [33]. After trial and error, albumin was identified as a suitable second linker. Binding L-glutamic acid to nHA slightly improved water dispersibility, and chemical bonding of albumin further enhanced it. The improved dispersibility of nHA in the aqueous phase increased the reactivity of the primary amino group of CFAS with the carboxy group of nHA-G [12]. Chemical bonding between the CFAS surface and nHA was confirmed through ATR-FTIR spectra, and the presence of nHA on the CFAS particle surface was directly confirmed using a scanning electron microscope [32].

Oliva et al. [34] compared the response of cultured human osteoblasts to five commercially used glass ionomer cements (Ketac-Fil Aplicap, lonocem lonocap 1.0, GC Fuji II, GC Fuji II LC, and Vitremer 3M). As a result, most glass ionomer cements tested showed biocompatibility, except for Vitremer 3M, and showed that they proliferated and expressed biochemical markers of osteoblast phenotype. As in the above study, Figure 8 of this study showed that osteoblasts were well spread on both GIC and GIC-nHA samples after 24 hours of culture. After culturing osteoblasts on the GIC and GIC-nHA discs for 24 and 48 hours, dead and live cells were observed using a confocal laser microscope. Staining with calcein-AM and ethidium homodimer III revealed that both GIC and GIC-nHA discs did not exhibit toxicity, as only live (green-stained) cells were observed (Figures 9 and 10). Additionally, more osteoblasts adhered to the GIC-nHA disc than to the GIC disc, likely due to the increased affinity for osteoblasts from the hydroxyapatite binding to the inorganic powder component of GIC. The MTT assay, performed after culturing osteoblasts on the GIC and GIC-nHA discs for 3 days, revealed greater cell proliferation on GIC-nHA compared to pristine GIC, attributable to nHA enhancing osteoblastic cell growth [35].

Von Kossa staining, used to quantify calcium-like mineralization in cell cultures, showed darker black images for the GIC-nHA disc compared to the GIC disc after 14 days of osteoblast culture (Figure 13). This suggests increased osteoblast affinity for GIC-nHA due to nHA on the CFAS surface [36, 37].

Future research should explore the long-term tissue compatibility of GIC-nHA in vivo to validate these findings. Additionally, varying the concentrations of nHA and exploring other potential linkers may further optimize the histocompatibility and mechanical properties of GIC. The development of GIC formulations tailored for specific dental applications could lead to broader clinical use and improved patient outcomes.

5. Conclusions

In conclusion, this study synthesized CFAS-nHA by chemically bonding nHA to the surface of CFAS, a silica-based solid particle. GIC-nHA was prepared by mixing CFAS-nHA with polyacrylic acid, a liquid component of Fuji II LC. Additionally, CFAS was mixed with the liquid components of Fuji II LC to prepare GIC. Culturing osteoblasts on GIC-nHA and GIC disks and examining cell activity and osteogenic potential revealed that GIC-nHA exhibited higher cell activity and osteogenic potential than GIC. This is attributed to nHA being chemically bonded to the surface of GIC's silica-based solid powder, promoting osteoblast activity. The method of chemically combining the surface of silica-based solid particles with nHA and using it as a GIC component can be an alternative to improve the histocompatibility of GIC.

Author Contributions: Conceptualization, S Kang; Data curation, SJ Park and I-K Kang; Formal analysis, SJ Park; Funding acquisition, S Kang; Investigation, SJ Park and S Kim; Methodology, S Kang, SJ Park, S Kim and I-K Kang; Resources, S Kim; Supervision, I-K Kang; Visualization, S Kang and I-K Kang; Writing – original draft, SJ Park and I-K Kang; Writing – review & editing, S Kang. All authors have read and agreed to the published version of the manuscript.

Acknowledgments: This work was supported by the 2023 Yeungnam University research grant (223A580032).

Conflicts of Interest: The authors declare no conflict of interest. The funders had no role in the design of the study, such as the collection, analyses, or interpretation of data, writing of the manuscript, or the decision to publish the results.

References

1. Sharanbir, K.S.; John, W.N. A review of glass-ionomer cements for clinical dentistry. *J. Funct. Biomater.* **2016**, *7*, 16. doi:10.3390/jfb7030016.
2. Farahnaz, S.; Ali, A.A.; Saba, S.; Mina, S. Comparison of shear bond strength of three types of glass ionomer cements containing hydroxyapatite nanoparticles to deep and superficial dentin. *J. Dent.* **2020**, *21*, 132–140.
3. Maja, B.P.; Valentina, B.R.; Ana, I.; Ana, P.; Sevil, G.; Ivana, M. Mechanical properties of glass ionomer cements after incorporation of marine derived hydroxyapatite. *Materials* **2020**, *13*, 3542. doi:10.3390/ma13163542.
4. Amin, F.; Rahman, S.; Khurshid, Z.; Zafar, M.S.; Sefat, F.; Kumar, N. Effect of nanostructures on the properties of glass ionomer dental restoratives/cements: A comprehensive narrative review. *Materials* **2021**, *14*, 6260. doi:10.3390/ma14216260.
5. Arita, K.; Yamamoto, A.; Shinonaga, Y.; Harada, K.; Abe, Y.; Nakagawa, K.; Sugiyama, S. Hydroxyapatite particle characteristics influence the enhancement of the mechanical and chemical properties of conventional restorative glass ionomer cement. *Dent. Mater. J.* **2011**, *30*, 672–683.
6. Mohd Pu'ad, N.A.S.; Abdul Haq, R.H.; Mohd, N.; Abdullah, H.Z.; Idris, M.I.; Lee, T.C. Synthesis method of hydroxyapatite: A review. *Materials Today: Proceedings* **2020**, *29*, 233–239.
7. Haider, A.; Haider, S.; Han, S.S.; Kang, I.-K. Recent advances in the synthesis, functionalization and biomedical applications of hydroxyapatite: a review. *RSC Adv.* **2017**, *7*, 7442–7458.
8. Sadat-Shojai, M.; Khorasani, M.T.; Dinpanah-Khoshdargi, E.; Jamshidi, A. Synthesis methods for nanosized hydroxyapatite with diverse structures. *Acta Biomater.* **2013**, *9*, 7591–7621.
9. Kang, I.G.; Park, C.I.; Lee, H.; Kim, H.E.; Lee, S.M. Hydroxyapatite microspheres as an additive to enhance radiopacity, biocompatibility and osteoconductivity of poly(methylmethacrylate) bone cement. *Materials* **2018**, *11*, 258. doi:10.3390/ma11020258.
10. Praveen, B.; Attiguppe, R.P.; Nadig, B. An in vitro comparative evaluation of compressive strength and antibacterial activity of conventional GIC and hydroxyapatite reinforced GIC in different storage media. *J. Clin. Diagn. Res.* **2015**, *9*, ZC51–ZC55.
11. Haider, A.; Gupta, K.C.; Kang, I.K. Morphological effects of HA on the cell compatibility of electrospun HA/PLGA composite nanofiber scaffolds. *Biomed. Res. Int.* **2014**, *2014*, 11. doi:10.1155/2014/308306.
12. Park, S.J.; Gupta, K.C.; Kim, H.; Kim, S.; Kang, I.-K. Osteoblast behaviours on nanorod hydroxyapatite-grafted glass surfaces. *Biomater. Res.* **2019**, *23*, 28. doi:10.1186/s40824-019-0178-6.
13. Khiri, M.Z.A.; Matori, K.A.; Zaid, M.H.M.; Abdullah, A.C.; Zainuddin, N.; Jusoh, W.N.W.; Jalil, R.A.; Rahman, N.A.A.; Kul, E.; Wahab, S.A.A.; Effendy, N. Soda lime silicate glass and clam shell act as precursor in synthesize calciumfluoroaluminosilicate glass to fabricate glass ionomer cement with different ageing time. *J. Mater. Res. Tech.* **2020**, *9*, 6125–6134.
14. Jia, S.; Liu, Y.; Ma, Z.; Liu, C.; Chai, J.; Li, Z.; Song, W.; Hu, K. A novel vertical aligned mesoporous silica coated nanohydroxyapatite particle as efficient dexamethasone carrier for potential application in osteogenesis. *Biomed. Mater.* **2021**, *16*, 035030. doi:10.1088/1748-605X/abcae1.
15. Aykol, M.; Montoya, J.H.; Hummelshøj, J. Rational solid-state synthesis routes for inorganic materials. *J. Am. Chem. Soc.* **2021**, *143*, 9244–9259.
16. Haider, A.; Versace, D.; Gupta, K.C.; Kang, I.-K. Pamidronic acid-grafted nHA/PLGA hybrid nanofiber scaffolds suppress osteoclastic cell viability and enhance osteoblastic cell activity. *J. Mater. Chem. B* **2016**, *4*, 7596.
17. Kamiya, H.; Iijima, M. Surface modification and characterization for dispersion stability of inorganic nanometer-scaled particles in liquid media. *Sci. Tech. Adv. Mater.* **2010**, *11*, 044304. doi:10.1088/1468-6996/11/4/044304.
18. Kwon, G.; Kim, H.; Gupta, K.C.; Kang, I.-K. Enhanced tissue compatibility of polyetheretherketone disks by dopamine-mediated protein immobilization. *Macromol. Res.* **2018**, *25*, 128–138.
19. Xing, Z.-C.; Han, S.-J.; Shin, Y.-S.; Koo, T.-H.; Moon, S.; Jeong, Y.; Kang, I.-K. Enhanced osteoblast responses to poly(methyl methacrylate)/hydroxyapatite electrospun nanocomposites for bone tissue engineering. *J. Biomater. Sci. Polym. Ed.* **2013**, *24*, 61–76. doi:10.1163/156856212X623526.
20. Tiernan, H.; Byrne, B.; Kazarian, S.G. ATR-FTIR spectroscopy and spectroscopic imaging for the analysis of biopharmaceuticals. *Spectrochim Acta A Mol Biomol Spectrosc.* **2020**, *241*, 118636.
21. Alhazmi, H.A. FT-IR spectroscopy for the identification of binding sites and measurements of the binding interactions of important metal ions with bovine serum albumin. *Sci. Pharm.* **2019**, *87*, 5. doi:10.3390/scipharm87010005.
22. Park, S.J.; Kim, B.S.; Gupta, K.C.; Lee, D.Y.; Kang, I.-K. Hydroxyapatite nanorod-modified sand blasted titanium disk for endosseous dental implant applications. *Tissue Eng. Regen. Med.* **2018**, *15*, 601–614. doi: 10.1007/s13770-018-0151-9
23. Haider, A.; Kim, S.; Huh, M.-W.; Kang, I.-K. BMP-2 grafted nHA/PLGA hybrid nanofiber scaffold stimulates osteoblastic cells growth. *Biomed. Res. Int.* **2015**, *2015*, 281909. doi:10.1155/2015/281909.

 doi:10.20944/preprints202406.1757.v1

24. Fletcher, D.A.; Mullins, R.D. Cell mechanics and the cytoskeleton. *Nature* **2010**, *28*, 485–492. doi:10.1038/nature08908.
25. Tayalia, P.; Mooney, D.J. Controlled growth factor delivery for tissue engineering. *Adv. Mater. (Weinheim, Ger.)* **2009**, *21*, 3269–3285.
26. Moshaverinia, A.; Ansari, S.; Moshaverinia, M.; Roohpour, N.; Darr, J.A.; Rehman, I. Effects of incorporation of hydroxyapatite and fluoroapatite nanobioceramics into conventional glass ionomer cements (GIC). *Acta Biomater.* **2008**, *4*, 432–440.
27. Bilić-Prcić, M.; Brzović Rajić, V.; Ivanišević, A.; Pilipović, A.; Gurgan, S.; Miletić, I. Mechanical Properties of Glass Ionomer Cements after Incorporation of Marine Derived Hydroxyapatite. *Materials (Basel)* **2020**, *13*, 3542.
28. Barandehfard, F.; Kianpour Rad, M.; Hosseinnia, A.; Khoshroo, K.; Tahriri, M.; Jazayeri, H.E.; Moharamzadeh, K.; Tayebi, L. The addition of synthesized hydroxyapatite and fluorapatite nanoparticles to a glass-ionomer cement for dental restoration and its effects on mechanical properties. *Ceram. Int.* **2016**, *42*, 17866-17875.
29. Noorani, T.Y.; Luddin, N.; Ab. Rahman, I.; Masudi, S.M. In vitro cytotoxicity evaluation of novel nano-hydroxyapatite-silica incorporated glass ionomer cement. *J. Clin. Diagn. Res.* **2017**, *11*, ZC105–ZC109.
30. Stanislawski, L.; Daniau, X.; Lautié, A.; Goldberg, M. Factors responsible for pulp cell cytotoxicity induced by resin-modified glass ionomer cements. *J. Biomed. Mater. Res.* **1999**, *48*, 277–288.
31. Kwon, Y.D.; Yang, D.H.; Lee, D.W. A titanium surface-modified with nano-sized hydroxyapatite and simvastatin enhances bone formation and osseointegration. *J. Biomed. Nanotech.* **2015**, *11*, 1007–1015.
32. Kim, H.; Lee, Y.H.; Kim, N.K.; Kang, I.K. Bioactive surface of zirconia implant prepared by nano-hydroxyapatite and type I collagen. *Coatings* **2022**, *12*, 1335.
33. Kang, S.; Haider, A.; Gupta, K.C.; Kim, H.; Kang, I. Chemical bonding of biomolecules to the surface of nano-hydroxyapatite to enhance its bioactivity. *Coatings* **2022**, *12*, 999. doi:10.3390/coatings12070999.
34. Oliva, A.; Della Ragione, F.; Salerno, A.; Riccio, V.; Tartaro, G.; Cozzolino, A.; D'Amato, S.; Pontoni, G.; Zappia, V. Biocompatibility studies on glass ionomer cements by primary cultures of human osteoblasts. Biomater. 1996, 17, 1351–1356.
35. Kumar, D.; Gittings, J.P.; Turner, I.G.; Bowen, C.R.; Bastida-Hidalgo, A.; Cartmell, S.H. Polarization of hydroxyapatite: Influence on osteoblast cell proliferation. *Acta Biomater.* **2010**, *6*, 1549–1554.
36. Schneider, M.R. Von Kossa and his staining technique. *Histochem. Cell Biol.* **2021**, *156*, 523–526.
37. Chen, C.S.; Chang, J.H.; Srimaneepong, V.; Wen, J.Y.; Tung, O.H.; Yang, C.H.; Lin, H.C.; Lee, T.H.; Han, Y.; Huang, H.H. Improving the in vitro cell differentiation and in vivo osseointegration of titanium dental implant through oxygen plasma immersion ion implantation treatment. *Surf. Coat. Technol.* **2020**, *399*, 126125.